Study of the role of oxygen in the evolution of red wine colour under different ageing conditions in barrels and bottles

Rosario Sánchez-Gómez[a], Maria del Alamo-Sanza*[a], Víctor Martínez-Martínez[b] and Ignacio Nevares*[b]

[a] Department of Analytical Chemistry, [b] Department of Agricultural and Forestry Engineering, UVaMOX-Group, Universidad de Valladolid, 34001 Palencia, Spain

*maria.delalamo.sanza@uva.es *ignacio.nevares@uva.es

Abstract

Wine ageing in barrels is conditioned, among other factors, by the amount of oxygen received during this process, which thus impacts its final properties. The aim of this study was to evaluate the effect of oxygen on wine colour during ageing in barrels and bottles during different times. The use of barrels with different and known rates of oxygenation allows the effect of different oxygenation conditions throughout the process in barrels and its later evolution in bottles. A simulation process of ageing in bottles was used to study the impact of bottling in wines after differing ageing periods in barrels. The study of wine´s oxygen consumption capacity has been tied to colour modifications during ageing in barrels and bottles. Wines aged in barrels with a high oxygenation rate showed greater avidity to consume oxygen taking less time to consume that available, which is reflected in a greater increase in colour intensity.

Keywords: *barrel OTR, bottle storage simulation, colour, oxygen consumption kinetics, red wine, vis spectroscopy*

1. Introduction

Oxygen is an essential parameter to be taken into account during red wine ageing in barrels, since it determines the reactions that occur between the compounds of the wine and those provided by the wood during this process (polymerisation of tannins and anthocyanins, consumption of free sulphur dioxide, oxidation of ethanol to acetaldehyde, modifications in the aromatic profile of the wine...), and consequently directly affects the final properties of the wine. Therefore, the interaction between ageing wine and oxygen determines the process and the reactions that occur need to be understood (Cano-López, López-Roca, Pardo-Minguez, & Gómez Plaza, 2010; del Alamo-Sanza & Nevares, 2017; del Alamo, Nevares, Gallego, Fernández de Simón, & Cadahía, 2010). The barrel acts as an active vessel that allows the transfer of oxygen to the wine being aged (del Alamo-Sanza & Nevares, 2017), and that amount of oxygen is known as the oxygen transfer rate (OTR), which defines the oxygen reaching the wine through the joints between the staves and throughout the wood as the main oxygen pathways (del Alamo-Sanza & Nevares, 2017; Nevares Domínguez & del Alamo-Sanza, 2014). The OTR of the oak wood used to make barrels depends on its species, geographical origin, density, anatomical properties and cooperage process, among others (Nevares et al., 2019). For a long time, the choice of oak barrels for wine ageing has been based on the type of oak and also its grain. Recently, Martínez-Martínez et al. (2019) have proposed a non-destructive method to classify staves according to their wood OTR in order to build barrels with low and high oxygenation rates. It has been demonstrated that it is possible to make barrels with a high OTR, dosing the wine with more than twice the oxygen provided by barrels with a low OTR (Prat-García, Nevares, Martínez-Martínez, & del Alamo-Sanza, 2020).

Colour is one of the most important characteristics in red wines (Heras-Roger, Díaz-Romero, & Darias-Martín, 2016). In addition to being one of the first attributes to be appreciated by the consumer, its stability during vinification and ageing can help to monitor wine quality, so it is used as an age marker in wine (Atanasova, Fulcrand, Cheynier, & Moutounet, 2002). Although colour is determined by many variables present throughout all the vinification process (grape variety, yeast strain used during fermentation, among others), during wood and bottle ageing storage conditions one of the most influential factors is oxygen. During wine ageing oxygen determines the formation of pigments derived from anthocyanins and polymerized pigments, which leads to an increase in intensity and colour stability (Heras-Roger et al., 2016). As wood ageing progresses, the concentration of anthocyanins and copigments decreases due to the occurrence of various chemical reactions, resulting in the decreased influence of copigmentation on wine colour expression. However, the number of new pigments derived from chemical reactions continues to increase and is becoming increasingly important in modifying red wine colour during ageing (Es-Safi & Cheynier, 2009). The change from red purple to brick red hues is attributed to the progressive formation of new pigments, since anthocyanins react with other compounds (Es-Safi & Cheynier, 2009; Fulcrand, Dueñas, Salas, & Cheynier, 2006; Wang, Race, & Shrikhande, 2004). After barrel ageing, a bottle period is fundamental since wines undergo changes that entail a continuation of those processes that begin during ageing in wood, which are determined not only by their initial wine characteristics but also by those of the wood and the length of the contact period (Guadalupe & Ayestarán, 2008). In relation to colour, the most important phenomenon includes increased colour stability, since polymerisation reactions have continued, showing a more stable colour, which could be a result of the beneficial effects of compounds extracted from the wood (Oberholster et al., 2015).

Due to the importance of oxygen on wine evolution, several works have focused on the study of the effect of oxygen addition during bottling, in most cases reducing the bottling volume in order to amplify the oxidation phenomena (Caillé et al., 2010). There are several factors that have been taken into account: different amounts of oxygen (Carrascón et al., 2018; Marrufo-Curtido, Carrascón, Bueno, Ferreira, & Escudero, 2018; Petrozziello et al., 2018; Ugliano et al., 2012), providing oxygen in different consecutive cycles (Carrascón, Bueno, Fernandez-Zurbano, & Ferreira, 2017; Gambuti, Picariello, Rinaldi, & Moio, 2018) and also, oxygen exposures at different temperatures and times (Oliveira, Barros, Silva Ferreira, & Silva, 2015). From among the ageing of wine bottle variables under study, temperature exerts a significant effect on the kinetics of the reactions occurring during ageing (Scrimgeour, Nordestgaard, Lloyd, & Wilkes, 2015). Several works have been and are being carried out with the aim of studying the ageing process using higher temperatures than usual for bottle ageing, in order to accelerate the processes that bottled wine undergoes due to the temperature-dependent rates for different wine ageing reactions (Giuffrida de Esteban et al., 2019; Hopfer, Buffon, Ebeler, & Heymann, 2013). However, no approximations have been revealed between the simulated time with temperature and the real time under normal ageing conditions.

The main purpose of this work is to study the effect of the oxygenation level on red wine, on its colour evolution during ageing in French oak barrels and its later storage in bottles. The use of barrels with a known oxygenation level has allowed the effect on wine colour at different ageing times in barrels and bottles to be verified.

2. Materials and Methods

2.1. Wine samples and barrels

A young red wine produced on an industrial scale in 2017 belonging to the Spanish appellation of origin Ribera del Duero was used. The chemical parameters of the wine before ageing were: total acidity 4.56 g/L (expressed as tartaric acid), volatile acidity 0.48 g/L (expressed as acetic acid), sugars 1.4 g/L, degree strength 15.16%, colour intensity 15, and total polyphenol index 61. For ageing, 8 French oak barrels (*Quercus petraea* Liebl.) with a capacity of 225-L and different OTR were used: 4 barrels with low OTR (from now on, L-OTR) and another 4 with high OTR (henceforth, H-OTR). For their construction a protocol is fully described in a previous study (Prat-García et al., 2020), a seasoned stave classification method based on the anatomical features of the wood by means of image analysis and artificial neuronal network (Martínez-Martínez et al., 2019) was used. The oxygen rate of the 4 H-OTR barrels was over twice that of the 4 L-OTR ones (Prat-García et al., 2020).

The wine was transferred into the barrels at the same moment and stored during the ageing period in the same ageing room in the experimental cellar at the University of Valladolid (Palencia, Spain), where humidity and temperature conditions were controlled at 65–75 % and 15–16 ºC. Samples from each barrel were taken every three months using an inert sample-taking method, always maintaining a nitrogen atmosphere around the bung hole. In order to profile their colour evolution throughout one year, 8 wine samples were studied every 3 months (4 from L-OTR barrels and 4 from H-OTR barrels) up to 12 months during ageing, so a total of 32 wines (labelled as *Initial, I*) were sampled (Figure 1S).

2.2. Oxygen consumption kinetics and data analysis

The oxygen consumption rate (OCR) of the wines from different oxygenation scenarios was evaluated as defined by Nevares et al. (2017) as they had been subjected to different ageing times (3, 6, 9 and 12 months) in high and low oxygenation barrels. Thus, atmospheric air saturation processes were performed on the *Initial (I)* wines from each of the barrels (4 from L-OTR barrels and 4 from H-OTR barrels) and at each sampling time (3, 6, 9 and 12 months), 32 wines in total (8 x 4) (Figure 1S). Once the wines were air saturated to study the oxygen consumption kinetics, 4 mL were transferred to four SensorVials SV-PSt5 for each wine sample (PreSens Precision Sensing GmbH, Regensburg, Germany). The oxygen consumption kinetics were then carried out in quadruplicate, measuring dissolved oxygen (DO) in a multi SDR SensorDish Reader device (PreSens Precision Sensing GmbH, Regensburg, Germany) ensuring that all samples were measured simultaneously in the same conditions. The DO of the samples was measured every hour throughout the consumption process, producing a total of 128 wine oxygen consumption kinetics (32 x 4) (Figure 1S). The wine samples obtained after oxygen consumption were labelled as *final consumption (FC).*

To study the oxygen consumption kinetics, the curve data were pre-processed in order to obtain 32 final curves: one for each sample. To this end, the first step was to remove the initial data before the maximum value and the final data after the time with a derivative value greater than zero considering a one-hour window of time. This procedure removes the possible initial noise of the DO readings and the final static values. After that, the four consumed oxygen kinetics measured for each wine sample were analysed and the remaining curves averaged in order to obtain the mean oxygen kinetic curve for each sample. Several fitting models have been proposed by other authors (Ferreira, Carrascon, Bueno, Ugliano, & Fernandez-Zurbano, 2015; Marrufo-Curtido et al., 2018), although in this study the curves were fitted with a phenomenological equation (1) developed in previous work (Nevares et al., 2017),

$$O_2(t) = \frac{a}{1 + b \cdot e^{c \cdot t}} \qquad (1)$$

where t is the time in hours, e refers to the exponential function and a, b and c are the parameters of the phenomenological equation. Finally, parameters presented in Table 1S were extracted from each kinetic curve for their later analysis. Briefly, the total consumption process time (t_{end}) defines the total time that the wine needs to consume the oxygen it is capable of consuming, this being lower for samples that were able to consume the oxygen faster. The Area Under the Curve (AUC) is the integral under the kinetic curve and is lower for the samples that consume the oxygen quickly but also for the samples that are able to reach a final oxygen value lower than others. The minimum value of the first derivative (min_der), as an absolute value, is a parameter that shows the maximum consumption velocity of the sample, so the slower consumption samples are expected to have a lower value for the min_der parameter than the faster consumption ones. Oxygen at half the consumption time (oxy_mid) shows the oxygen level in the middle of the consumption process, giving an idea of the convexity of the kinetic curve, this being lower for the samples that were able to consume more oxygen in the first half of the time period, that is, samples with a high oxygen avidity at the beginning of the oxygen consumption process. Finally, the t_{OCRI} parameter (Nevares et al., 2017) is the time where the area under the curve is half of the total AUC, this being greater for the samples with a slow oxygen consumption rate or for samples that are not capable of consuming all the oxygen dissolved in the air.

2.3. Bottle simulation conditions

In order to study the effect of oxygen in the bottle period of the red wines subjected to different ageing times in barrels, the samples collected after 3, 6, 9 and 12 months underwent two periods in bottles. It was decided to do this in small volumes taken from the samplings carried out to avoid modifying the good development of ageing in barrels.

To simulate the ageing time in bottle and once the follow-up of the oxygen consumption kinetic had finished, wine samples were stored under two different temperature conditions in 25 mL screwcap airtight bottles, taking the temperature as the modulating parameter of the ageing time in bottle (unpublished works). The Short Bottle Ageing Simulation time (*SBAS*) of the *final consumption (FC)* wines was done by storing the containers at 15ºC for 35 days and the Long Bottle Ageing Simulation (*LBAS*) by storing them at 35 ºC for 35 days, all in a controlled temperature chambers.

2.4. Real bottle conditions

After one year of ageing in barrels, the wine was bottled to go through its ageing period in the bottle. For this, after the last sampling was carried out (12 month), all the wines were bottled using 750 mL bottles in the winery, for which a semi-automatic monoblock with filler and corker "modello 97/M4" (Officine Pesce, Bubbio, Italy) were used. Before that, and to reproduce the real winery situation, wines from the barrels from the same OTR (4 L-OTR and 4 H-OTR barrels) were mixed and labelled as L-OTR-MIX and H-OTR-MIX. Sübr closures (Vinventions Deutschland GmbH, Fußgönheim, Germany) were used. All bottles were stored in the same bottle room under controlled humidity (65–75 %) and temperature (15–16 ºC) conditions. After 4 months in bottle, 5 bottles of each type (L-OTR and H-OTR) were opened and analysed.

2.5. Visible spectrum measurement and data analysis

The visible spectra were analysed in a total of 130 wine samples: from each of the 4 barrel ageing times (3, 6, 9 and 12 months), each of the 8 barrels (4 with L-OTR and 4 with H-OTR) and each sampling moment (*I*, *FC*, *SBAS* and *LBAS*) (4 x 8 x 4), in addition to the two wines from the real bottle conditions (Figure 1S). The visible spectrum of every wine sample was measured in duplicate using quartz cells with a path-length of 1 mm and a PerkinElmer's LAMBDA 25 UV/vis Spectrophotometer (Waltham, MA, USA) interfaced to a computer. The spectra of all samples were obtained by measuring the absorbance in the range of 320 – 780 nm at 5 nm intervals. Pure water was used for the reference scan. The first step of the spectral signal processing was to average the signals of the two measurements of each situation, since a total of 260 signals were obtained. Moreover, the average of the 4 L-OTR and the 4 H-OTR barrels were also calculated respectively for each situation for the graphical representation and the comparison between them.

The accepted colour analysis for red wines is that made by measurements at three wavelengths, 420, 520 and 620 nm, and the calculations of colour intensity (sum of these absorbances as defined by (Glories, 1984); and tone as the ratio of absorbance at 420 to 520 nm) provide a useful method to describe wine colour. The CIELab space has been used to describe wine colour using all visible spectra. CIELab parameters were calculated using the "Method OIV-MA-AS2-11: Determination of chromatic characteristics according to CIELab" (OIV, 2006). These parameters were: L*, describing the lightness from black to white; b*, from blue to yellow; a*, from red to green; C*, chroma or saturation; and H*, hue angle.

To calculate the relative gains of the different bottle ageing simulation times (FC, $SBAS$ and *LBAS*) the difference between the absorbance at the time of study and the absorbance at the previous bottle time was divided by the absorbance at the previous bottle time. Thus, the relative gain for the *FC* bottle time was obtained considering the *Initial* spectrum as the previous time and the relative gain for the *SBAS* and *LBAS* bottle times were calculated considering *FC* as the previous time.

2.6. Statistical analysis

Regression and analysis of variance (ANOVA) at an alpha level of 5% with Fisher's least significant difference were carried out using the Statgraphics Centurion statistical program (version 18.1.12; StatPoint, Inc., VA, USA).

3. Results and Discussion

3.1. Kinetics of oxygen consumption

Figure 1 represents the mean consumption curves obtained after this processing procedure (section 2.2) and the error bars related to the standard deviation of the four replicates. The fitting curves employed to obtain the phenomenological equation parameters had a R^2 between 0.9629 and 0.9999 (Nevares et al., 2017). Table 1 summarized the 1-way ANOVA tests performed on the parameters that define the wine oxygen consumption kinetic curves in order to evaluate the significance of the differences between the barrel OTRs (L-OTR and H-OTR) considering the barrel ageing time (3, 6, 9 and 12 months). After six months of barrel ageing, the AUC parameter was significantly higher in wines from L-OTR barrels, which means less eagerness to consume oxygen and/or it is not able to consume all of its dissolved oxygen. After nine months of barrel ageing min_der was significantly lower in wines from H-OTR barrels, thus indicating a lower avidity for oxygen. Regarding the oxy_mid, it was significantly higher in wines from L-OTR barrels in the samples of the first half of the year in barrel. However, in the last sampling, H-OTR wine presented the highest value, which means that in the first half of the year of ageing, wines from L-OTR were less avid to consume oxygen, although at the end of the ageing this trend changes and these same wines showed a statistically significant higher avidity for oxygen consumption.

On the other hand, 1-way ANOVA tests were performed with wines from each barrel OTR (L-OTR and H-OTR) to evaluate the differences among the oxygen consumption kinetics of the barrel ageing times (Table 2). For t_{end} and t_{OCRI} the same significant differences were observed for samples after 3 and 6 months and those after 9 and 12 months for both OTR barrels, except for t_{OCRI} in wines from L-OTR sampled after 9 months. This indicates that in the first half of the barrel ageing period all the wines presented a greater avidity and oxygen consumption capacity, which slowed down towards the end of the year of barrel ageing. Analysing the oxy_mid parameter, there were no significant differences when considering the H-OTR samples, but in the case of those from L-OTR ones an increase in the capacity of oxygen consumption when wines have high levels of DO was observed as the barrel ageing time progressed. Finally, min_der also showed significant differences for both OTR barrel groups: both, L-OTR and H-OTR samples had an oxygen consumption maximum speed higher for the samples after 3 months and lower for the rest. Thus, the behaviour throughout the barrel ageing period differed according to barrel OTR. More specifically, wines aged in L-OTR barrels presented two moments of maximum initial avidity followed by moments in which this decreased, while those in H-OTR barrels after 3 months of ageing presented the maximum oxygen consumption speed when it was present in high concentrations with a strong decrease after 6 months. However, that avidity gradually recovered over ageing time with high oxygen contents. This result indicates that wines are more avid for oxygen in the first months of barrel ageing, and the wine-wood-oxygen interaction reactions give rise to compounds that are more stable and more resistant to oxidation in the following months. Furthermore, bearing in mind that in the first months of barrel ageing wines receive a significant dose of oxygen (between 30 and 40 % of the oxygen they are to receive during a year) (del Alamo-Sanza & Nevares, 2014), and which is higher in wines aged in H-OTR barrels (Prat-García et al., 2020), the more oxygen the wines have at their disposal, the higher the speed of oxygen consumption.

3.2. Visible spectra study

Spectral information of the wines from the L-OTR and H-OTR barrels after 3, 6, 9 and 12 months of barrel ageing are shown in Figure 2. Each graph in Figure 2 presents the data of one of these four barrel ageing times, where 8 spectral signals can be seen reflecting the average of the wines from the 4 barrels with the same OTR. Table 2 shows the relative gains calculated for some wavelengths among those that define colour intensity in red wines (420, 520 and 620 nm), analysing the different barrel ageing times of the two different oxygenation levels (L-OTR and H-OTR) for each bottle ageing simulation (*FC*, *SBAS* and *LBAS*).

After 3 months of barrel ageing the *FC* wines suffered an absorbance increase for all the wavelengths (Figure 2a), with a mean gain of around 40% compared to the *Initial* situation (Table 2), the increase in the L-OTR wines being higher than in those from H-OTR barrels (Table 2). The same was observed after 6 months of ageing (Figure 2b), but with a mean gain 10% lower than in the previous ageing period. Finally, after 9 and 12 months of barrel ageing (Figures 2c and 2d, respectively) the wines presented the greatest mean increments with 55% and 89%, respectively. Moreover, these increments were significantly higher in the H-OTR wine samples compared with that of the L-OTR ones for all the wavelengths analysed after 12 months of ageing, but not at 470 and 520 nm after 9 months. In contrast, there were no significant differences between the two oxidation levels for the samples after 3 and 6 months (Table 2). This confirms that the amount of oxygen received by the wine causes a significant increase in colour, increasing with the ageing time in barrels and with this increment being greater for wines from L-OTR barrels (Table 1).

Several authors reported the importance of adding small doses of oxygen to increase or modify the colouring matter (Atanasova et al., 2002) especially during the wine ageing process (Cano-López et al., 2010), because controlled oxygenation improves the final wine quality since it stabilizes colour. The wine spectrum was observed to suffer no significant change with the storage time in barrels. However, after subjecting the wines to a saturation and oxygen consumption process, the time periods in barrels can be differentiated (Figure 2). This result could be related to the chemical structure of the wine, which is defined by the compounds released by the oak wood and the interactions of these compounds with the wine (del Alamo-Sanza & Nevares, 2017). These processes, which are affected by the oxygen received by the wine during ageing in the different oxidation barrels, is also reflected in the capability of the wine to generate more stable compounds that appear after an air saturation process. Thus, the results obtained suggest that the generation of new pigments and the compounds extracted during the ageing process make the wine colour more stable after forced oxidation, showing a colour intensity gain that is significantly higher when barrel ageing time increases (Figure 2 and Table 2). Thus, *FC* wines presented an increase in the absorbance at 620 nm, being greater for longer barrel ageing times, which means a higher effect on the compounds related to the purple hue promoted by air saturation. This effect is linked to an increase in absorbance at 420 and 520 nm, which could be explained by the increase in some pigments of the A and B type vitisins groups (He et al., 2012). This evolution of the wine from red to purple was previously described for red wine subject to lower but constant oxygen doses over longer periods of time by micro-oxygenation techniques (Atanasova et al., 2002; del Alamo et al., 2010). Moreover, anthocyanin–alkyl/aryl–flavanol pigment compounds have been linked to the red-purple colours of wine that appear during the maturation stages (Pissarra et al., 2004), these pigments being responsible for the generation of the pyranoanthocyanin-flavanol compounds that can be found in red wine during ageing (Francia-Aricha, Guerra, Rivas-Gonzalo, & Santos-Buelga, 1997).

Analysing the differences between the two bottle simulation times, *SBAS* and *LBAS*, a great dependency on the barrel ageing time was seen (Figure 2 and Table 2). A decrease in the wavelength range between 370 and 470 nm and an increment in the range between 520 and 620 nm was observed for both L-OTR and H-OTR wines with 3 months of barrel ageing stored at *SBAS*, with no significant differences among them (Table 2). These results show the continuation in the evolution of colour during bottle storage time, generating compounds related to red and blue hues. This process could be favoured by the copigmentation processes, and also related to the loss of monomeric anthocyanin, which interacts with other wine compounds, causing the generation of other coloured compounds during the ageing process (Fernandes, Oliveira, Teixeira, Mateus, & de Freitas, 2016; He et al., 2012). Nevertheless, *SBAS* wines with 6, 9 and 12 months of barrel ageing reduced their absorbance in the wavelength range between 520 and 670 nm, being lower in H-OTR wines compared to L-OTR ones after 9 and 12 months of barrel ageing. This means that the instability of the wines increased with the barrel ageing time, which suggests that the compounds formed are favoured by forced air saturation, more numerous when the ageing time increases, and were more unstable during the *SBAS*, causing more losses in the absorbance wavelengths related to red and purple. These results can be linked to colour stabilization during the oxidation process and also to the phenolic compound reactions in different ways (Atanasova et al., 2002). Thus, oxidation eases the formation in the first period of anthocyanin-flavanol derived purple compounds linked by ethyl bridges, (Es-Safi & Cheynier, 2009) and intensely coloured at wine pH. After that, the formation of several pyranone–anthocyanin compounds are formed, whose more stable forms have yellow and orange hues (pyranone–anthocyanin), with λ_{max} ~370 nm. The first ones (anthocyanin-flavanol pigments) are very unstable in wine (He et al., 2012), which causes the pyranone–anthocyanin to gradually dominate, contributing to the colour modification to orange and yellow, which is related to a more evolved aged red. Nevertheless, the absorbance decreases in the wavelength range of the red and purple colours (520-620 nm) were not associated with an absorbance increase in the wavelengths related to yellow and orange hues (370-470 nm), so a continuous loss was observed, this being greater in wines with more barrel ageing time.

Focusing on the *LBAS* wines, several spectral differences can be observed when comparing with *SBAS* ones (Figure 2), because this longer bottle time caused the development of brown hues. Wines from L-OTR and H-OTR barrels stored at *LBAS* after 3 months of barrel ageing showed an increment in the wavelength ranges of 350 – 520 nm and 620 – 670 nm, mainly because of anthocyanin loss, flavonol oxidation and new compound formation. In this case, the small decrease in absorbance at 570 nm could be associated with a loss of vinylpyranoanthocyanins (also known as portisins) and normally generated due to the reaction of a type A vitisin with flavanols in the presence of acetaldehyde (Mateus, Silva, Rivas-Gonzalo, Santos-Buelga, & De Freitas, 2003), which are characterized by having a blue hue in high-pH solutions (with a λ_{max} ~570 nm). After 6 and 9 months of barrel ageing, *LBAS* wines showed similar results: an absorbance loss at 520 and 575 nm, with no significant differences between L-OTR and H-OTR wines and an absorbance increase in the 350-470 nm range and at 620 nm, with a mean gain of 10% and 3.5%, respectively, in relation to *FC*. Moreover, these absorbance increases were significantly greater for the L-OTR wines in comparison with the H-OTR ones. Finally, *LBAS* wines with a year of barrel ageing presented a general absorbance decrease for both L-OTR and H-OTR wines, this being greater in the range between 520 nm and 670 nm, which is related to larger losses of the red and purple compounds (Escribano-Bailón, Álvarez-García, Rivas-Gonzalo, Heredia, & Santos-Buelga, 2001). This suggests that the colour increase recorded in the *FC* wines is not stable during the bottle storage time. The small absorbance losses at 520 nm could be explained by the greater colour stabilization caused by the copigmentation phenomena. Nevertheless, it is interesting to emphasize that colour intensity was higher for *Initial* wines. For this reason, it could be said that, regardless of the barrel ageing time, wine colour first changed from red to purple and then to yellow and orange hues as a consequence of the ageing conditions. To conclude, it has been seen that barrel oxygenation (L-OTR or H-OTR) affects the characteristics of the wine (Table 2): in general, wine aged in H-OTR barrels showed greater variations in the spectra compared with L-OTR ones, with higher losses or smaller increases for both bottle ageing conditions (*SBAS* and *LBAS*), except for *LBAS* wines with 3 and 6 months of barrel ageing. In addition, as mentioned above, H-OTR wines had a higher oxygen consumption speed (Table 1), that is, showed more oxygen avidity, which seems to result in less generation of stable compounds.

3.3. Colour parameter relationships

The results of the relationships between the different colour parameters are presented in Figure 3 and Table 2S. This analysis has been performed for all the different barrel ageing periods (3, 6, 9 and 12 months) and for each bottle ageing time (*I*, *FC*, *SBAS* and *LBAS*). Results showed that L* (lightness) was inversely proportional to colour intensity (CI) (Figure 3a): it decreases with the creation of new pigments and increases CI. It is interesting to note that, for the *Initial* wines, small modifications in CI cause the greater changes in L* compared to the rest of the bottle ageing stages (*FC*, *SBAS* or *LBAS*), which can be seen in the regression equation (Table 2S). This relationship has been analysed by several authors, finding that L* can be transformed in the better-known and appreciated standard parameter CI (Casassa & Sari, 2007). Thus, Almela et al. (1995) found a correlation coefficient of -0.957 and Esparza, (2006) recorded similar results. As previously described (section 3.2.), *FC* wines showed a significant increase in CI, reflecting a relationship similar to that obtained for the *SBAS* wines, which means that in both cases L* was similarly affected by the CI changes. This could be observed by their similar smaller slopes, indicating that they were the least affected by the CI changes, whereas wines from *LBAS* presented an intermediate scenario.

Initial wines were those with higher C* levels (Figure 3b). Moreover, the CI increase associated with barrel ageing time was significantly related to the reduction of the wine vivacity (Table 2S, slope -3.667, $R^2 = 0.9544$), as other authors described (Almela et al., 1995; Casassa & Sari, 2007;

Esparza, 2006; Gil-Muñoz, Gómez-Plaza, Martínez, & López-Roca, 1997). It has been seen that oxidation processes facilitate the reduction of the C* parameter and the increase of CI, which means a loss in the wine colour vivacity, with a better correlation for *FC* wines (Table 2S, C* = -4.956 · CI + 115.170, R^2 = 0.9822). Nevertheless, there was an increase of C* during the *SBAS*, with a corresponding CI decrease, while after the *LBAS* the wines increased CI, maintaining an inverse relation with C* (Table 2S). The H* (hue) parameter had a very significant relationship with CI when *Initial* wines were considered (Table 2S and Figure 3c). H* decreased when CI increased and, because of that, and in accordance with the previous observations, the increases in CI related to the ageing process also caused a reduction in L*. In addition, small CI increases caused significant decreases in H*, due to the greater increment of yellow pigments compared with that of red ones. This suggests that the formation of yellow and orange stable compounds, such as pyranone–anthocyanin ones (He et al., 2012), is greater than that of those responsible for the red colour. Nevertheless, as previously mentioned, dosing high levels of oxygen also caused the formation of new red and blue hue pigments (Es-Safi & Cheynier, 2009) and, because of that, the relationship between H* and CI in the wines after the air saturation process (*FC*, *SBAS* or *LBAS*) was weaker (Table 2S, R^2 = 0.5612, R^2 = 0.5236 and R^2 = 0.6164, respectively) than that described for the *Initial* ones. Conversely, in the same way as what happened with wine vivacity C*, for *FC* wines a small increment in H* could be observed, which was lower for *LBAS*. When comparing the relationship between the L* loss and the H* increment, similar results were obtained, because the correlation between both was positive and significant in the *Initial* wines (Table 2S). For this reason, barrel ageing time was related to a loss of L* and a decrease in H* (Figure 3d), but this did not happen in the stages after the air saturation process. These results do not agree with other authors (Gil-Muñoz et al. 1997), who obtained a negative correlation between these parameters.

A positive and significant correlation between L* and a* (redness) for the *Initial* wines was observed (Figure 3e and Table 2S). The evolution of wines during the two bottle times (*SBAS* and *LBAS*) showed that L* loss was related to a smaller decrease in a* (the slope of the regression equation was 0.1490, 0.1665 and 0.1452 for the *FC*, *SBAS* and *LBAS* wines, respectively Table 2S). This trend was also found by Gil-Muñoz et al., (1997) in experiments where wines with low L* were analysed, and by Esparza (2006), who found a stronger relationship among both parameters (r=0.905) when analysing red wines, though these results do not agree with the results reported by Almela et al. (1995). The a* parameter shows the influence of the red and green colour range in red wine, where a high level of this parameter indicates the importance of the red hues. Wines with greater CI were observed to show the lower a* values, which were the samples associated with the *FC* wines and the subsequent bottle ageing periods (*SBAS* and *LBAS*) (Figure 3f). For this reason, the greater CI compared with the *Initial* wines is reflected in the lower level of the a* parameter for the *FC* wines. The correlations between the absorbance at 520 nm and 370 nm reflect the importance of the pyranone–anthocyanin compounds, the yellow and orange hues being more predominant than the red ones. These compounds had their maximum absorbance wavelength at ~370 nm, (He et al., 2012). The relation between these absorbances was A370 = 1.108 *A520, $R^2 = 0.9933$, with a lower correlation after the bottle ageing period, with slopes lower than those for the *SBAS* (0.565) or *LBAS* (0.293) wines (Table 2S). The b* parameter shows the influence of the yellow-blue hues in wine colour, the higher values being associated with important brown hues and values close to or lower than 0 related to blue. The red wines analysed obtained a regression graph for the b*-CI very similar to the L*-CI. It was because L* is related to the Y CIELab coordinate and b* is related to both Y and Z CIELab coordinates, but for the wines studied in this work the Z value was almost zero for all samples, which meant that the correlation between L* and b* was very close to 1. Moreover, it has been seen that wines with a higher CI belong to the *FC* wine samples, which also had lower values of b*. This result suggests that the larger compounds formed after the air saturation procedure when compared with the *Initial* wines produced important blue tones which were reduced with the CI decrease for the *SBAS* wines. Furthermore, after the *SBAS* period the importance of the yellow component increased, but then, after the *LBAS* period, the blue component dominated wine colour again. There was also a significant correlation between the b* parameter and absorbance at 320 nm (Figure 3g and Table 2S), with the *Initial* wines having a greater blue component and a lower b* value, thus verifying the previous comments. After the air saturation procedure (*FC*) and the bottle ageing process (*SBAS* and *LBAS*), the colour intensity increment caused by the generation of new compounds was reflected in a greater increase for absorbance at 620 nm compared with yellow wavelength absorbance (Figure 3h and Table 2S). The same behaviour could be seen when analysing the red wavelength (Table 2S) with a regression equation of A520 = 1.537 · A620 + 5.022, $R^2 = 0.9892$ for the *FC* wines and A520 = 1.117 · A620 + 6.06, $R^2 = 0.2252$ for *SBAS* ones. Nevertheless, when analysing the long bottle ageing simulation time (*LBAS)*, blue colour loss was related to a greater increment of the yellow and red wavelengths (Table 2S). This observation shows the instability of the purple colour compounds that were present in the *FC* wines.

3.4. Kinetics and CIELab relations

Initial and *FC* spectral wine information and their relationship with the oxygen consumption kinetics parameters were studied. Analysing the *Initial* wine spectra, only min_der had a R^2 greater than 0.35 when doing a correlation analysis with the spectral parameters. The best correlation was obtained with the absorbance at 670 nm (correlation coefficient of -0.6418, *p-value* = $7.53 \cdot 10^{-5}$). This relationship was lower than zero, which means that wines with a high oxygen consumption avidity (high min_der), have a low absorbance at 670 nm, and therefore less red and blue hues.

For the *FC* wine spectra, four parameters had a R^2 greater than 0.35: $min\_der, AUC,$ $t_{end}, and\ t_{OCRI}$. The best correlation (correlation coefficient of 0.7845, *p-value* = $1.08 \cdot 10^{-7}$) was obtained between min_der and H*, which means that wines with a low oxygen consumption speed were expected to have a lower H*, causing the wines to have more blue and less yellow hues. The correlation between t_{end} and b* and L* (correlation coefficients of -0.6687 and -0.5515, respectively, *p-value* = $2.87 \cdot 10^{-5}$ and $1.07 \cdot 10^{-3}$) suggests that wines with greater yellow component and lightness will need less time to consume the oxygen available.

Finally, the absolute gain between the *Initial* and *FC* spectral parameters was also evaluated and three parameters had a R^2 greater than 0.35: t_{end}, oxy_mid and t_{OCRI}. The best correlation was obtained between t_{end} and a* variation (correlation coefficient of -0.6953, *p-value* = $1.00 \cdot 10^{-5}$), indicating that wines that need more time to consume the available oxygen show a smaller redness increment.

3.5. Approximation of bottled simulation to a real situation

Figure 4 shows the comparison between spectral data of wines after 12 barrel ageing months that were bottled in winery conditions and stored at 15-16 ºC for 4 months (labelled MIX) and the wines with simulated bottled times: *SBAS* and *LBAS*. It can be seen that the spectral data of the MIX samples of both L-OTR and H-OTR wines were close to the *SBAS* spectral data. L-OTR-MIX and H-OTR-MIX wines showed a small absorbance increment between 350 and 420 nm and a small decrease between ranges 350 – 420 nm and 450 – 530 nm when compared with the *SBAS* wines. This means that L-OTR-MIX and H-OTR-MIX wines were more evolved than the *SBAS* ones, where some compounds with red and purple hues were replaced by other compounds with yellow and orange ones. So, related to the spectral properties, the short bottle ageing simulation (*SBAS*) seems to be similar to a wine bottled for 4 months under real conditions. Moreover, spectral information data of L-OTR-MIX and H-OTR-MIX wines were very similar, which also occurred with the *SBAS* wines (Figure 2). This result would mean that from a spectral properties point of view the wines from L-OTR and H-OTR barrels can be differentiated by their ageing time in bottle.

4. Conclusions

The oxygen consumed by the wine during its storage in barrels with different oxygenation rates determines colour evolution in the bottle period. Wine significantly increased the absorbances related to less stable compounds (blue or purple tones) for longer periods and more oxygen in barrel ageing, but as bottle ageing progresses the absorbances associated with yellow and orange hues prevailed. Equally, for the bottled simulation conditions studied, short bottle ageing simulation (*SBAS*) and long bottle ageing simulation (*LBAS*), the results depended on barrel ageing time and also the barrel oxygenation level (L-OTR or H-OTR). Although wines from barrels with different oxygenation rates tend to be similar after a first simulated period in the bottle (*SBAS*), it was observed that they differentiated again when time in the bottle was extended (*LBAS*). *LBAS* wines were characterized by a greater evolution, related to the increase in yellow and loss of purple tones, more evident in wines from H-OTR barrels which showed the highest oxygen avidity.

Finally, keeping the wines at 15 ºC for 35 days (*SBAS*) after air saturation showed spectral profiles similar to those aged for 4 months in real bottle ageing conditions. These first results of the bottling simulation methodology used seem promising enough to initiate new studies that will allow longer stays in the bottle to be reproduced.

Acknowledgements

This study was financed by MINECO (AGL2017-87373-C3-2-R project) and Junta de Castilla y León (VA315P18 project), R.S.-G. Post-doctoral contract from Junta de Castilla y León and V.M.M. post-doctoral contract from Interreg Spain-Portugal (Iberphenol project). The authors wish to thank Ann Holliday for her services in revising the English and to INTONA cooperage for their collaboration in oak wood selection and toasting.

Declaration of Competing Interest

The authors declare that they have no known competing financial interests or personal relationships that could have appeared to influence the work reported in this paper.

References

Almela, L., Javaloy, S., Fernández-López, J. A., & Lôpez-Roca, J. M. (1995). Comparison between the tristimulus measurements Yxy and L*a*b* to evaluate the colour of young red wines. *Food Chemistry*, *53*(3), 321–327. https://doi.org/10.1016/0308-8146(95)93940-S

Atanasova, V., Fulcrand, H., Cheynier, V., & Moutounet, M. (2002). Effect of oxygenation on polyphenol changes occurring in the course of wine-making. *Analytica Chimica Acta*, *458*(1), 15–27. https://doi.org/10.1016/S0003-2670(01)01617-8

Caillé, S., Samson, A., Wirth, J., Diéval, J. B., Vidal, S., & Cheynier, V. (2010). Sensory characteristics changes of red Grenache wines submitted to different oxygen exposures pre and post bottling. *Analytica Chimica Acta*, *660*(1–2), 35–42. https://doi.org/10.1016/j.aca.2009.11.049

Cano-López, M., López-Roca, J. M., Pardo-Minguez, F., & Gómez Plaza, E. (2010). Oak barrel maturation vs. micro-oxygenation: Effect on the formation of anthocyanin-derived pigments and wine colour. *Food Chemistry*, *119*(1), 191–195.

Carrascón, V., Bueno, M., Fernandez-Zurbano, P., & Ferreira, V. (2017). Oxygen and SO2Consumption Rates in White and Rosé Wines: Relationship with and Effects on Wine Chemical Composition. *Journal of Agricultural and Food Chemistry*, *65*(43), 9488–9495. https://doi.org/10.1021/acs.jafc.7b02762

Carrascón, V., Vallverdú-Queralt, A., Meudec, E., Sommerer, N., Fernandez-Zurbano, P., & Ferreira, V. (2018). The kinetics of oxygen and SO2 consumption by red wines. What do they tell about oxidation mechanisms and about changes in wine composition? *Food Chemistry*,

241, 206–214. https://doi.org/10.1016/j.foodchem.2017.08.090
Casassa, F., & Sari, S. (2007). Aplicación Del Sistema Cie-Lab a Los Vinos Tintos. Correlación Con Algunos Parámetros Tradicionales. *Revista Enología*, *5*(May-Jun), 1–15. Retrieved from http://www.researchgate.net/profile/L_Casassa/publication/259582055_APLICACIN_DEL_SISTEMA_CIE-LAB_A_LOS_VINOS_TINTOS_CORRELACIN_CON_ALGUNOS_PARMETROS_TRADICIONALES/links/02e7e52cc2f09291a3000000.pdf
del Alamo-Sanza, M., & Nevares, I. (2014). Recent advances in the evaluation of the oxygen transfer rate in oak barrels. *Journal of Agricultural and Food Chemistry*, *62*(35), 8892–8899. https://doi.org/10.1021/jf502333d
del Alamo-Sanza, M., & Nevares, I. (2017). Oak wine barrel as an active vessel: A critical review of past and current knowledge. *Critical Reviews in Food Science and Nutrition*, *58*(16), 2711–2726. https://doi.org/10.1080/10408398.2017.1330250
del Alamo, M., Nevares, I., Gallego, L., Fernández de Simón, B., & Cadahía, E. (2010). Micro-oxygenation strategy depends on origin and size of oak chips or staves during accelerated red wine aging. *Analytica Chimica Acta*, *660*(1–2), 92–101. https://doi.org/10.1016/j.aca.2009.11.044
Es-Safi, N.-E., & Cheynier, V. (2009). Flavanols and Anthocyanins as Potent Compounds in the Formation of New Pigments during Storage and Aging of Red Wine. In *Red Wine Color* (ACS Sympos, pp. 143–159). https://doi.org/10.1021/bk-2004-0886.ch009
Escribano-Bailón, T., Álvarez-García, M., Rivas-Gonzalo, J. G., Heredia, F. J., & Santos-Buelga, C. (2001). Color and stability of pigments derived from the acetaldehyde-mediated condensation between malvidin 3-O-glucoside and (+)-catechin. *Journal of Agricultural and Food Chemistry*, *49*(3), 1213–1217. https://doi.org/10.1021/jf001081l
Esparza, I. S. J. . F. J. (2006). Chromatic characterisation of three consecutive vintages of. *Analytica Chimica Acta*, *563*, 331–337.
Fernandes, A., Oliveira, J., Teixeira, N., Mateus, N., & de Freitas, V. (2016). A review of the current knowledge of red wine colour. *Journal International Des Sciences de La Vigne et Du Vin*, *51*(1), 1–21.
Ferreira, V., Carrascon, V., Bueno, M., Ugliano, M., & Fernandez-Zurbano, P. (2015). Oxygen Consumption by Red Wines. Part I: Consumption Rates, Relationship with Chemical Composition, and Role of SO2. *Journal of Agricultural and Food Chemistry*, *63*(51), 10928–10937. https://doi.org/10.1021/acs.jafc.5b02988
Francia-Aricha, E. M., Guerra, M. T., Rivas-Gonzalo, J. C., & Santos-Buelga, C. (1997). New anthocyanin pigments formed after condensation with flavanols. *Journal of Agricultural and Food Chemistry*, *45*(6), 2262–2266. https://doi.org/10.1021/jf9609587
Fulcrand, H., Dueñas, M., Salas, E., & Cheynier, V. (2006). Phenolic Reactions during Winemaking

and Aging. *American Journal of Enology and Viticulture*, *3*(57), 289–297. Retrieved from http://search.ebscohost.com/login.aspx?direct=true%7B&%7Ddb=bth%7B&%7DAN=31767783%7B&%7Dsite=ehost-live

Gambuti, A., Picariello, L., Rinaldi, A., & Moio, L. (2018). Evolution of Sangiovese wines with varied tannin and anthocyanin ratios during oxidative aging. *Frontiers in Chemistry*, *6*, 1–11. https://doi.org/10.3389/fchem.2018.00063

Gil-Muñoz, R., Gómez-Plaza, E., Martínez, A., & López-Roca, J. M. (1997). Evolution of the CIELAB and other spectrophotometric parameters during wine fermentation. Influence of some pre and postfermentative factors. *Food Research International*, *30*(9), 699–705. https://doi.org/10.1016/S0963-9969(98)00029-5

Giuffrida de Esteban, M. L., Ubeda, C., Heredia, F. J., Catania, A. A., Assof, M. V., Fanzone, M. L., & Jofre, V. P. (2019). Impact of closure type and storage temperature on chemical and sensory composition of Malbec wines (Mendoza, Argentina) during aging in bottle. *Food Research International*, *125*(May). https://doi.org/10.1016/j.foodres.2019.108553

Glories, Y. (1984). La couleur des vins rouges 2. Mesure, origine et interprétation. *OENO One*, *18*, 253–271.

Guadalupe, Z., & Ayestarán, B. (2008). Changes in the color components and phenolic content of red wines from Vitis vinifera L. Cv. “Tempranillo” during vinification and aging. *European Food Research and Technology*, *228*(1), 29–38. https://doi.org/10.1007/s00217-008-0902-2

He, F., Liang, N. N., Mu, L., Pan, Q. H., Wang, J., Reeves, M. J., & Duan, C. Q. (2012). Anthocyanins and their variation in red wines II. Anthocyanin derived pigments and their color evolution. *Molecules*, *17*(2), 1483–1519. https://doi.org/10.3390/molecules17021483

Heras-Roger, J., Díaz-Romero, C., & Darias-Martín, J. (2016). What Gives a Wine Its Strong Red Color? Main Correlations Affecting Copigmentation. *Journal of Agricultural and Food Chemistry*, *64*(34), 6567–6574. https://doi.org/10.1021/acs.jafc.6b02221

Hopfer, H., Buffon, P. A., Ebeler, S. E., & Heymann, H. (2013). The combined effects of storage temperature and packaging on the sensory, chemical, and physical properties of a cabernet sauvignon wine. *Journal of Agricultural and Food Chemistry*, *61*(13), 3320–3334. https://doi.org/10.1021/jf3051736

Marrufo-Curtido, A., Carrascón, V., Bueno, M., Ferreira, V., & Escudero, A. (2018). A procedure for the measurement of Oxygen Consumption Rates (OCRs) in red wines and some observations about the influence of wine initial chemical composition. *Food Chemistry*, *248*, 37–45. https://doi.org/10.1016/j.foodchem.2017.12.028

Martínez-Martínez, V., del Alamo-Sanza, M., & Nevares, I. (2019). Application of image analysis and artificial neural networks to the prediction in-line of OTR in oak wood planks for cooperage. *Materials & Design*, *181*, 107979. https://doi.org/10.1016/j.matdes.2019.107979

Mateus, N., Silva, A. M. S., Rivas-Gonzalo, J. C., Santos-Buelga, C., & De Freitas, V. (2003). A new class of blue anthocyanin-derived pigments isolated from red wines. *Journal of Agricultural and Food Chemistry*, *51*(7), 1919–1923. https://doi.org/10.1021/jf020943a

Nevares Domínguez, I., & del Alamo-Sanza, M. (2014). Oxygène et barriques: Actualisation des connaissances Quantité et voies de pénétration de l'oxygène dans la barrique. *Revue des oenologues et des techniques vitivinicoles et oenologicques*, *41*(153), 41–44.

Nevares, I., del Alamo-Sanza, M., Martínez-Martínez, V., Menéndez-Miguélez, M., Van den Bulcke, J., & Van Acker, J. (2019). Influence of Quercus petraea Liebl. wood structure on the permeation of oxygen through wine barrel staves. *Wood Research and Technology. Holzforschung*, *73*(9), 859–870. https://doi.org/10.1515/hf-2018-0299

Nevares, I., Martínez-Martínez, V., Martínez-Gil, A., Martín, R., Laurie, V. F., & del Álamo-Sanza, M. (2017). On-line monitoring of oxygen as a method to qualify the oxygen consumption rate of wines. *Food Chemistry*, *229*, 588–596. https://doi.org/10.1016/j.foodchem.2017.02.105

Oberholster, A., Elmendorf, B. L., Lerno, L. A., King, E. S., Heymann, H., Brenneman, C. E., & Boulton, R. B. (2015). Barrel maturation, oak alternatives and micro-oxygenation: Influence on red wine aging and quality. *Food Chemistry*, *173*, 1250–1258. https://doi.org/10.1016/j.foodchem.2014.10.043

OIV. (2006). Compendium of international analysis of methods – OIV Chromatic Characteristics. Retrieved October 31, 2019, from Method OIV-MA-AS2-11. website: http://www.oiv.int/public/medias/2478/oiv-ma-as2-11.pdf

Oliveira, C. M., Barros, A. S., Silva Ferreira, A. C., & Silva, A. M. S. (2015). Influence of the temperature and oxygen exposure in red Port wine: A kinetic approach. *Food Research International*, *75*, 337–347. https://doi.org/10.1016/j.foodres.2015.06.024

Petrozziello, M., Torchio, F., Piano, F., Giacosa, S., Ugliano, M., Bosso, A., & Rolle, L. (2018). Impact of increasing levels of oxygen consumption on the evolution of color, phenolic, and volatile compounds of Nebbiolo wines. *Frontiers in Chemistry*, *6*(APR), 1–15. https://doi.org/10.3389/fchem.2018.00137

Pissarra, J., Lourenço, S., González-Paramás, A. M., Mateus, N., Santos Buelga, C., Silva, A. M. S., & De Freitas, V. (2004). Structural characterization of new malvidin 3-glucoside-catechin aryl/alkyl-linked pigments. *Journal of Agricultural and Food Chemistry*, *52*(17), 5519–5526. https://doi.org/10.1021/jf0494433

Prat-García, S., Nevares, I., Martínez-Martínez, V., & del Alamo-Sanza, M. (2020). Customized oxygenation barrels as a new strategy for controlled wine aging. *Food Research International*, *131*(May), 108982. https://doi.org/10.1016/j.foodres.2020.108982

Scrimgeour, N., Nordestgaard, S., Lloyd, N. D. R., & Wilkes, E. N. (2015). Exploring the effect of elevated storage temperature on wine composition. *Australian Journal of Grape and Wine Research*, *21*, 713–722. https://doi.org/10.1111/ajgw.12196

Ugliano, M., Dieval, J., Siebert, T. E., Kwiatkowski, M., Aagaard, O., & Waters, E. J. (2012).

Oxygen Consumption and Development of Volatile Sulfur Compounds during Bottle Aging of Two Shiraz Wines. In fl uence of Pre- and Postbottling Controlled Oxygen Exposure. *Journal of Agricultural and Food Chemistry*, *60*, 8561−8570.

Wang, H., Race, E. J., & Shrikhande, A. J. (2004). Anthocyanin transformation in Cabernet Sauvignon wine during aging. *ACS Symposium Series*, *886*, 198–216. https://doi.org/10.1021/jf034501q

FIGURE CAPTIONS

Figure 1. Mean oxygen consumption kinetic curves of wines from both barrel oxygenation levels, low (L-OTR) and high (H-OTR) with an ageing time of a) 3 months; b) 6 months; c) 9 months; and d) 12 months.

Figure 2. Visible spectral information in wines from both barrel oxygenation levels, low (L-OTR) and high (H-OTR) at different study moments (initial, after oxygen consumption, short bottle ageing simulation and long bottle ageing simulation) with an ageing time of: a) 3 months; b) 6 months; c) 9 months; and d) 12 months.

Figure 3. Linear regressions for several pairs of spectral and CIELab parameters for wines at different study moments (initial, after oxygen consumption, short bottle ageing simulation and long bottle ageing simulation).

Figure 4. Visible spectral comparative between bottle simulation and real conditions for wines after 12 months of ageing.

TABLES

Table 1. Value of the parameters that define the oxygen consumption kinetic curves of wines from both barrel oxygenation levels, low (L-OTR) and high (H-OTR) for each barrel ageing time (3, 6, 9 and 12 months).

Table 2. Percentage of relative gain and/or loss of the selected wavelengths of the spectra made for wines from both barrel oxygenation levels, low (L-OTR) and high (H-OTR), each barrel ageing time (3, 6, 9 and 12 months) and each bottle ageing simulation moment (after oxygen consumption, short bottle ageing simulation and long bottle ageing simulation).

SUPPLEMENTARY MATERIAL

Figure 1S. Experimental design.

Table 1S. Parameters extracted from the oxygen consumption kinetic curves.

Table 2S. Regression equations and coefficient of determination (R^2) for several pairs of spectral and CIELab parameters considering the different moment of study.

Table 1. Value of the parameters that define the oxygen consumption kinetic curves of wines from both barrel oxygenation levels, low (L-OTR) and high (H-OTR) for each barrel ageing time (3, 6, 9 and 12 months).

Barrel time (months)	**Barrel oxygenation rate**	t_{end}	AUC	min_der	oxy_mid	t_{OCRI}
3	L-OTR	46.06 ± 0.13 a, A	2887 ± 388 a, A	16.49 ± 2.11 a, C	93.15 ± 4.44 b, C	11.06 ± 1.05 a, A
3	H-OTR	46.00 ± 0.00 a, α	2540 ± 127 a, α	18.16 ± 1.79 a, γ	77.44 ± 1.72 a, α	11.13 ± 0.32 a, α
6	L-OTR	45.06 ± 0.75 a, A	3114 ± 416 b, A	7.43 ± 3.07 a, A	83.93 ± 5.13 b, B	13.00 ± 1.37 a, A
6	H-OTR	44.50 ± 0.29 a, α	2562 ± 160 a, α	6.13 ± 0.19 a, α	75.24 ± 2.93 a, α	11.38 ± 0.48 a, α
9	L-OTR	75.31 ± 12.43 a, B	3173 ± 482 a, A	13.18 ± 1.77 b, B	74.73 ± 4.09 a, A	16.25 ± 2.84 a, AB
9	H-OTR	70.81 ± 9.51 a, β	2860 ± 422 a, α	7.78 ± 0.85 a, αβ	74.71 ± 2.29 a, α	14.63 ± 2.45 a, β
12	L-OTR	87.06 ± 22.32 a, B	3608 ± 953 a, A	7.79 ± 0.13 a, A	74.82 ± 1.46 a, A	19.88 ± 6.65 a, B
12	H-OTR	66.19 ± 6.47 a, β	3032 ± 319 a, α	8.55 ± 0.87 a, β	81.41 ± 4.82 b, α	14.94 ± 1.94 a, β

Barrel oxygenation rate: a) L-OTR: low oxygen transfer rate; and b) H-OTR: high oxygen transfer rate.

t_{end}: total consumption time (h); AUC: area under the curve (hPa·h); min_der: absolute value of the minimum of the first derivative (hPa/h); oxy_mid: oxygen at half consumption time (hPa); t_{OCRI}: time when the area under the kinetic curve is half the total area under the curve (h).For each parameter, different small letters indicate significant differences among barrel oxygenations for each bottle time, capital letters indicate significant differences among bottle times for wines aged in L-OTR barrels and Greek letters indicate significant differences among bottle times for wines aged in H-OTR barrels according to the Fisher's LSD test ($\alpha < 0.05$). The mean values are shown with their standard deviation.

Table 2. Percentage of relative gain and/or loss of the selected wavelengths of the spectra made for wines from both barrel oxygenation levels, low (L-OTR) and high (H-OTR), each barrel ageing time (3, 6, 9 and 12 months) and each bottle ageing simulation moment (after oxygen consumption, short bottle ageing simulation and long bottle ageing simulation).

Barrel time (months)	Bottle time	Barrel	λ (nm) 370	420	470	520	570	620	670	Colour intensity
3	FC	L-OTR	38.52 ± 6.95 a	41.55 ± 7.45 a	42.35 ± 7.48 a	37.84 ± 7.28 a	35.24 ± 7.35 a	41.96 ± 9.24 a	65.52 ± 15.05 a	39.79 ± 7.59 a
	FC	H-OTR	33.62 ± 3.07 a	36.54 ± 3.04 a	37.74 ± 3.37 a	33.96 ± 3.88 a	31.22 ± 4.00 a	36.96 ± 3.43 a	57.55 ± 5.41 a	35.34 ± 3.45 a
	SBAS	L-OTR	-3.88 ± 1.04 a	-1.17 ± 1.61 a	0.02 ± 1.22 a	3.62 ± 1.16 a	5.89 ± 1.61 a	3.96 ± 3.37 a	8.53 ± 10.99 a	1.81 ± 1.60 a
	SBAS	H-OTR	-4.22 ± 0.67 a	-1.58 ± 0.86 a	-0.32 ± 0.66 a	3.26 ± 0.81 a	5.40 ± 1.11 a	3.59 ± 1.37 a	7.41 ± 4.91 a	1.43 ± 0.82 a
	LBAS	L-OTR	13.78 ± 1.16 a	23.66 ± 1.90 a	18.84 ± 1.34 a	3.54 ± 0.63 a	-2.92 ± 1.08 a	24.41 ± 4.95 a	114.98 ± 23.50 a	14.05 ± 1.62 a
	LBAS	H-OTR	13.25 ± 2.13 a	23.27 ± 3.13 a	19.26 ± 2.35 a	4.37 ± 1.30 a	-2.49 ± 1.67 a	22.64 ± 5.82 a	104.90 ± 25.58 a	14.05 ± 2.54 a
6	FC	L-OTR	33.16 ± 4.91 a	34.31 ± 5.75 a	33.84 ± 5.70 a	29.02 ± 5.70 a	24.92 ± 5.66 a	31.59 ± 7.17 a	43.23 ± 12.84 a	31.42 ± 5.92 a
	FC	H-OTR	30.32 ± 7.04 a	30.60 ± 7.89 a	30.15 ± 7.89 a	25.59 ± 8.24 a	21.68 ± 8.13 a	26.45 ± 9.99 a	32.35 ± 16.96 a	27.64 ± 8.35 a
	SBAS	L-OTR	-6.69 ± 0.57 a	-4.86 ± 0.93 a	-3.73 ± 0.81 a	-1.14 ± 1.29 a	1.18 ± 2.02 a	-0.95 ± 3.21 a	0.08 ± 8.10 a	-2.59 ± 1.31 a
	SBAS	H-OTR	-6.75 ± 0.32 a	-5.11 ± 0.49 a	-3.83 ± 0.44 a	-1.05 ± 0.40 a	0.79 ± 0.32 a	-2.01 ± 0.86 a	-3.07 ± 3.56 a	-2.78 ± 0.47 a
	LBAS	L-OTR	8.43 ± 0.86 a	12.19 ± 0.35 a	7.00 ± 0.67 a	-4.89 ± 1.55 a	-13.27 ± 1.61 a	1.02 ± 1.86 a	41.77 ± 9.66 a	2.67 ± 0.72 a
	LBAS	H-OTR	9.75 ± 0.47 b	14.55 ± 0.43 b	8.72 ± 0.50 b	-3.94 ± 1.14 a	-11.66 ± 1.02 a	6.50 ± 1.19 b	62.70 ± 8.52 b	4.75 ± 0.44 b
9	FC	L-OTR	38.31 ± 5.22 a	43.37 ± 6.41 a	45.21 ± 6.60 a	43.02 ± 7.11 a	39.33 ± 7.43 a	46.41 ± 9.92 a	71.35 ± 23.34 a	43.59 ± 7.15 a
	FC	H-OTR	47.03 ± 4.79 b	54.23 ± 5.62 b	55.88 ± 5.89 a	54.56 ± 6.75 a	51.90 ± 6.97 b	64.30 ± 8.53 b	118.28 ± 20.94 b	55.70 ± 6.49 b
	SBAS	L-OTR	-8.54 ± 0.35 b	-7.27 ± 0.35 b	-5.87 ± 0.38 b	-2.08 ± 0.69 b	-0.07 ± 1.16 b	-3.42 ± 1.74 b	-9.19 ± 4.89 b	-4.30 ± 0.69 b
	SBAS	H-OTR	-11.03 ± 0.92 a	-10.64 ± 1.34 a	-9.02 ± 1.26 a	-5.56 ± 1.24 a	-4.52 ± 1.58 a	-10.09 ± 2.63 a	-23.04 ± 6.32 a	-8.18 ± 1.46 a
	LBAS	L-OTR	8.80 ± 0.84 b	14.27 ± 0.63 b	10.07 ± 0.95 b	-2.25 ± 1.39 a	-11.25 ± 0.99 a	2.51 ± 1.03 b	41.57 ± 9.02 b	4.89 ± 0.51 b
	LBAS	H-OTR	4.95 ± 1.09 a	9.69 ± 1.62 a	6.97 ± 1.44 a	-4.20 ± 1.33 a	-13.33 ± 1.70 a	-3.51 ± 3.77 a	15.30 ± 12.13 a	1.34 ± 1.75 a
12	FC	L-OTR	48.78 ± 5.30 a	58.04 ± 6.93 a	56.52 ± 6.90 a	51.77 ± 6.83 a	51.04 ± 7.12 a	78.59 ± 11.74 a	196.21 ± 34.34 a	57.73 ± 7.43 a
	FC	H-OTR	57.72 ± 3.91 b	70.72 ± 4.58 b	68.91 ± 4.74 b	64.34 ± 5.14 b	65.96 ± 5.11 b	104.37 ± 6.68 b	278.32 ± 14.89 b	72.04 ± 5.09 b
	SBAS	L-OTR	-16.50 ± 1.09 b	-17.91 ± 1.60 b	-15.22 ± 1.33 b	-12.01 ± 1.00 b	-12.93 ± 1.41 b	-24.90 ± 2.85 b	-52.29 ± 4.73 b	-16.24 ± 1.53 b
	SBAS	H-OTR	-19.36 ± 0.68 a	-21.61 ± 1.02 a	-18.61 ± 1.02 a	-15.23 ± 0.74 a	-17.11 ± 0.76 a	-31.37 ± 1.34 a	-60.64 ± 1.89 a	-20.21 ± 0.95 a
	LBAS	L-OTR	-3.58 ± 1.01 a	-3.16 ± 1.00 a	-4.42 ± 0.70 b	-13.55 ± 0.55 a	-24.41 ± 0.61 a	-26.47 ± 1.41 a	-41.65 ± 2.72 a	-11.36 ± 0.81 b
	LBAS	H-OTR	-4.98 ± 1.23 a	-4.84 ± 0.98 a	-6.09 ± 1.07 a	-15.08 ± 1.70 a	-25.77 ± 1.68 a	-28.08 ± 1.42 a	-42.50 ± 2.00 a	-13.06 ± 1.01 a

FC: after oxygen consumption; SBAS: short bottle ageing simulation; LBAS: long bottle ageing simulation. Wine ageing in barrel with: a) L-OTR: low oxygen transfer rate; H-OTR: high oxygen transfer rate.

For each wavelength, different letters indicate significant differences among barrel oxygenations for each bottle time according to the LSD test (α < 0.05). The mean values are shown with their standard deviation.

Figure 1. Mean oxygen consumption kinetic curves of wines from both barrel oxygenation levels, low (L-OTR) and high (H-OTR) with an ageing time of a) 3 months; b) 6 months; c) 9 months; and d) 12 months.

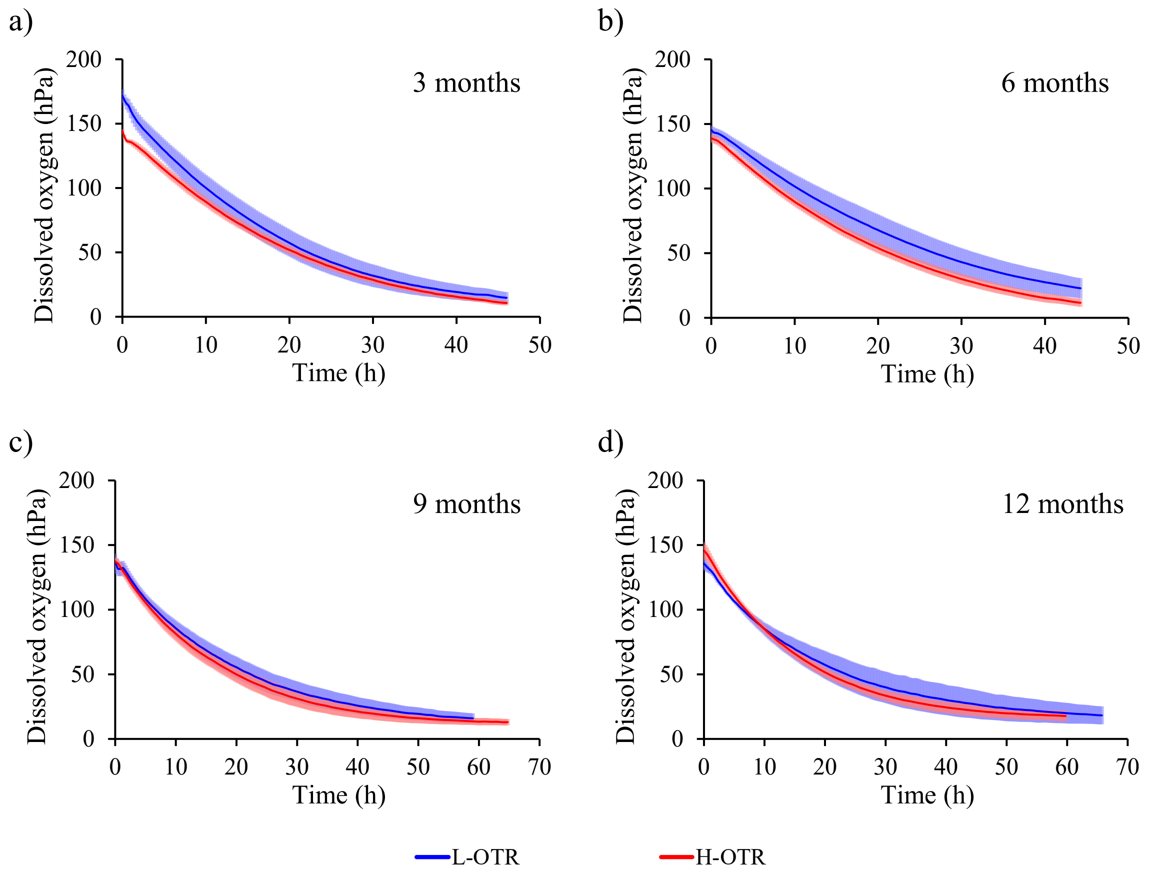

Figure 2. Visible spectral information in wines from both barrel oxygenation levels, low (L-OTR) and high (H-OTR) at different study moments (initial, after oxygen consumption, short bottle ageing simulation and long bottle ageing simulation) with an ageing time of a) 3 months; b) 6 months; c) 9 months; and d) 12 months.

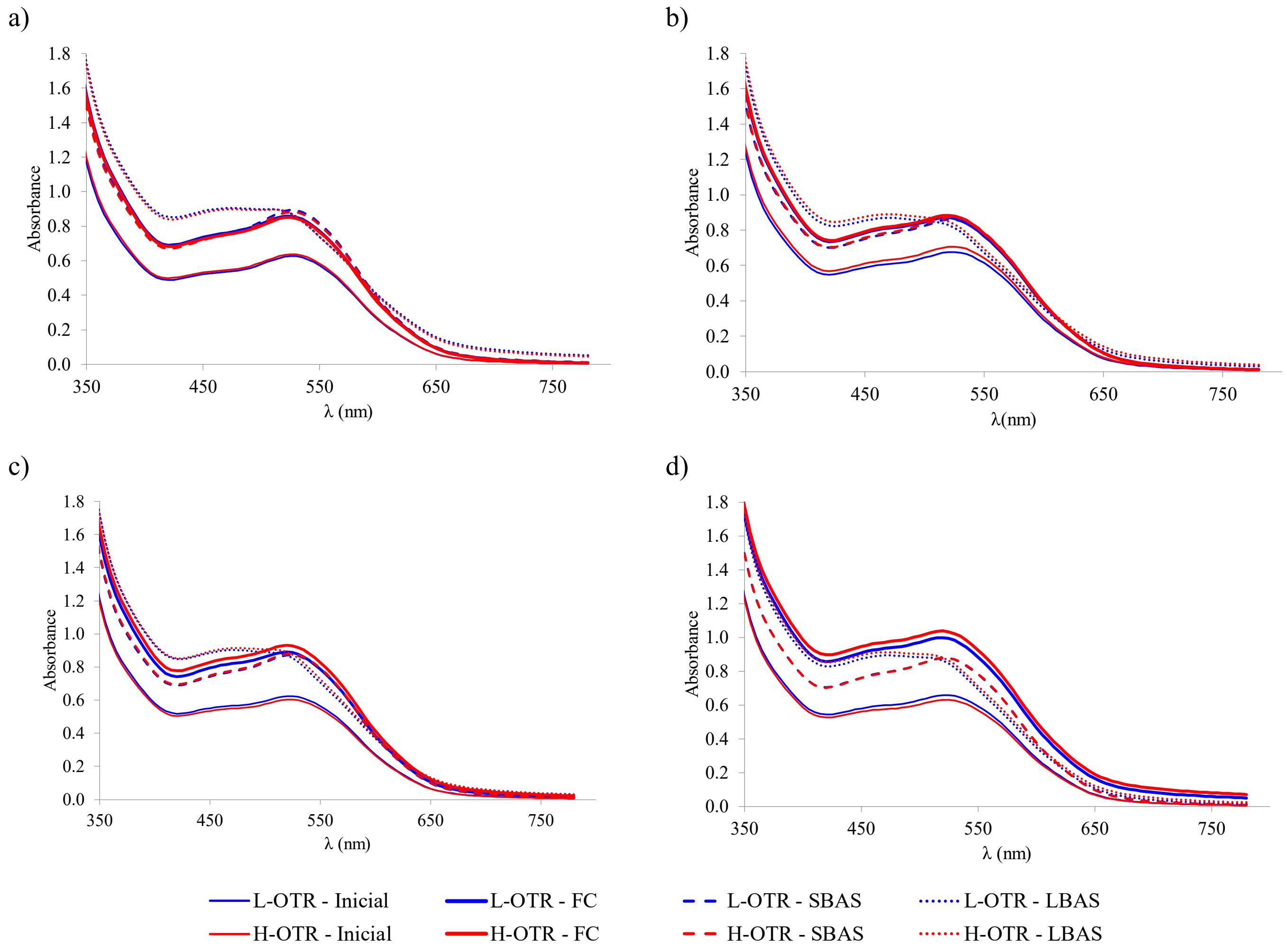

Figure 3. Linear regressions for several pairs of spectral and CIELab parameters for wines at different study moments (initial, after oxygen consumption, short bottle ageing simulation and long bottle ageing simulation).

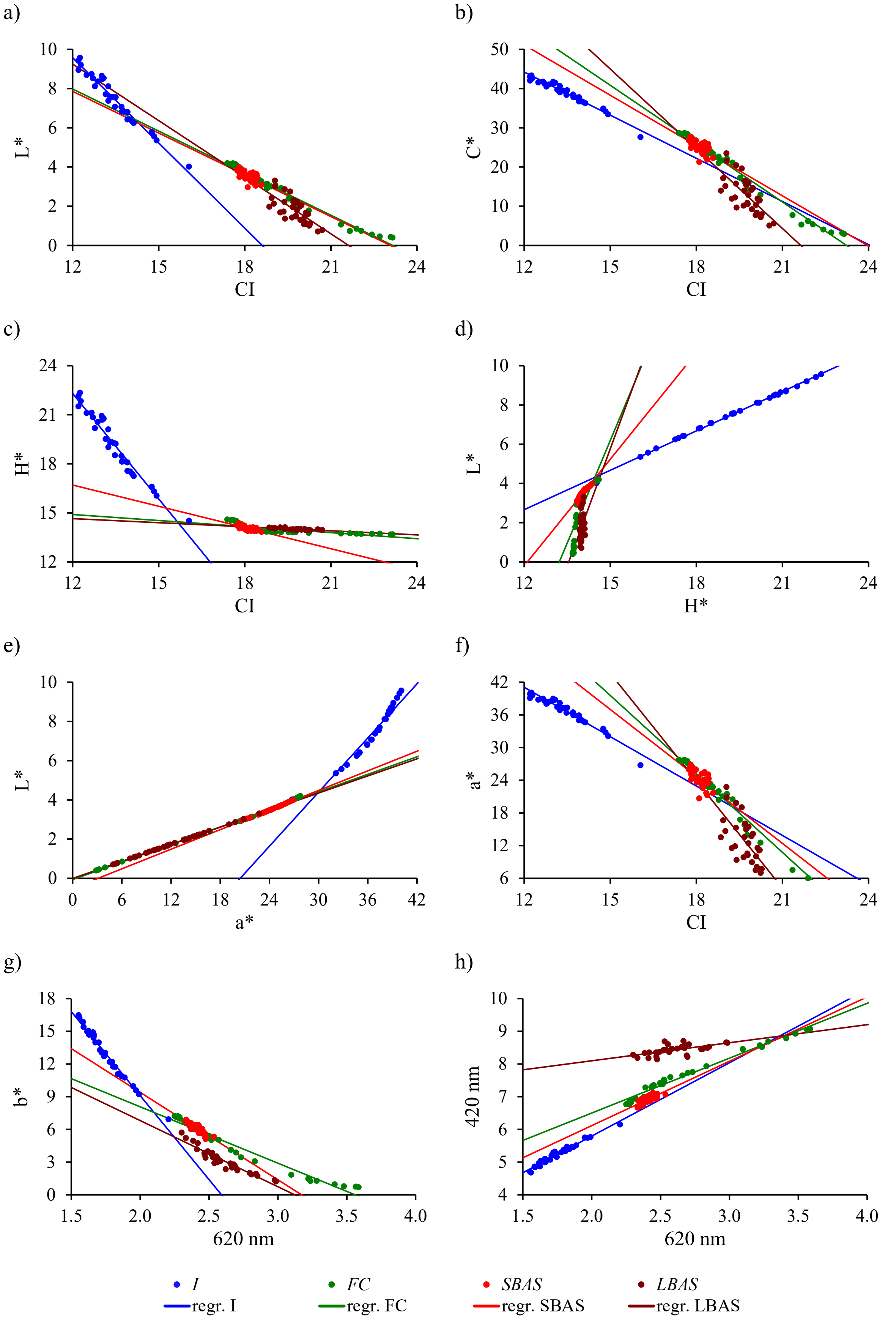

Figure 4. Visible spectral comparative between bottle simulation and real conditions for wines from 12 months of ageing.

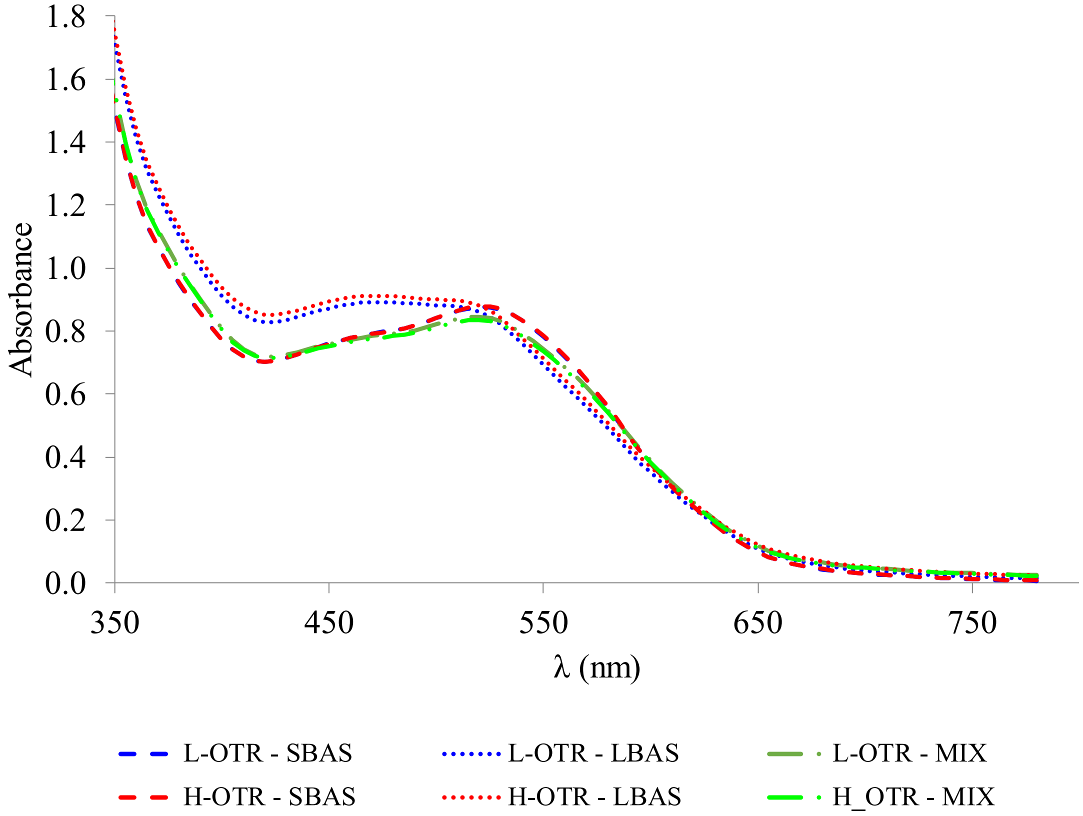

Table 1S. Parameters extracted from the oxygen consumption kinetic curves.

Name	Parameter	Name and equation/description
t_end	Total consumption time (h)	t_{end} : time of the last point of the oxygen curve
AUC	Area under the curve (hPa·h)	$AUC = \int_{t=0}^{t_{end}} O_2(t)dt$
min_der	Absolute value of the minimum of the first derivative (hPa/h)	$min\_der = \left\|min\left\{\frac{\partial\, O_2(t)}{\partial t}\right\}\right\|$
Oxy_min	Oxygen at half consumption time (hPa)	$oxy\_mid = O_2\left(t = {}^{t_{end}}/_{2}\right)$
t_{OCRI}	Time when the area under the kinetic curve is half the total area under the curve (h)	$t_{OCRI}\ so\ that\ \int_{t=0}^{t_{OCRI}} O_2(t)dt = \frac{1}{2}\cdot\int_{t=0}^{t_{end}} O_2(t)dt$

Table 2S. Regression equations and coefficient of determination (R^2) for several pairs of spectral and CIELab parameters considering the different moment of study.

	Initial wine (I)		***Final consumption wine (FC)***		***Short Bottle Simulation (SBAS)***		***Longt Bottle Simulation (LBAS)***	
	equation	R^2	*equation*	R^2	*equation*	R^2	*equation*	R^2
CI vs L*	L* = -1.448 · CI + 26.948	0.9575	L* = -0.715 · CI + 16.556	0.9784	L* = -0.709 · CI + 16.369	0.3888	L* = -0.961 · CI + 20.786	0.5127
CI vs C*	C* = -3.667 · CI + 88.214	0.9544	C* = -4.956 · CI + 115.170	0.9822	C* = -4.272 · CI + 102.373	0.3630	C* = -6.774 · CI + 146.587	0.5050
CI vs H*	H* = -2.150 · CI + 48.100	0.9485	H* = -0.123 · CI + 16.381	0.5612	H* = -0.433 · CI + 21.898	0.5236	H* = -0.083 · CI + 15.641	0.6164
H* vs L*	L* = 0.669 · H* - 5.370	0.9968	L* = 3.485 · H* - 46.085	0.6295	L* = 1.812 · H* - 21.953	0.9089	L* = 3.982 · H* - 53.962	0.0978
a* vs L*	L* = 0.460 · a* - 9.398	0.9383	L* = 0.149 · a* - 0.064	0.9978	L* = 0.167 · a* - 0.514	0.9968	L* = 0.145 · a* - 0.006	0.9999
CI vs a*	a* = -3.021 · CI + 77.315	0.9391	a* = -4.801 · CI + 111.576	0.9823	a* = -4.098 · CI + 98.465	0.3611	a* = -6.568 · CI + 142.139	0.5045
A520 vs A370	A370 = 0.847 · A520 + 2.974	0.9095	A370 = 1.108 · A520 + 1.737	0.9933	A370 = 0.565 · A520 + 5.74	0.4095	A370 = 0.293 · A520 + 10.022	0.1099
CI vs b*	b* = -2.493 · CI + 46.402	0.9575	b* = -1.233 · CI + 28.545	0.9784	b* = -1.223 · CI + 28.221	0.3888	b* = -1.658 · CI + 35.838	0.5127
A620 vs b*	b* = -15.415 · A620 + 39.931	0.9776	b* = -5.174 · A620 + 18.420	0.9649	b* = -8.022 · A620 + 25.44	0.7512	b* = -6.072 · A620 + 18.954	0.9083
A620 vs A420	A420 = 2.243 · A620 + 1.308	0.9638	A420 = 1.678 · A620 + 3.144	0.9810	A420 = 1.969 · A620 + 2.18	0.5435	A420 = 0.552 · A620 + 6.994	0.3741
A620 vs A520	A520 = 2.829 · A620 + 1.483	0.9306	A520 = 1.537 · A620 + 5.022	0.9892	A520 = 1.117 · A620 + 6.06	0.2252	A520 = 0.772 · A620 + 6.681	0.3323

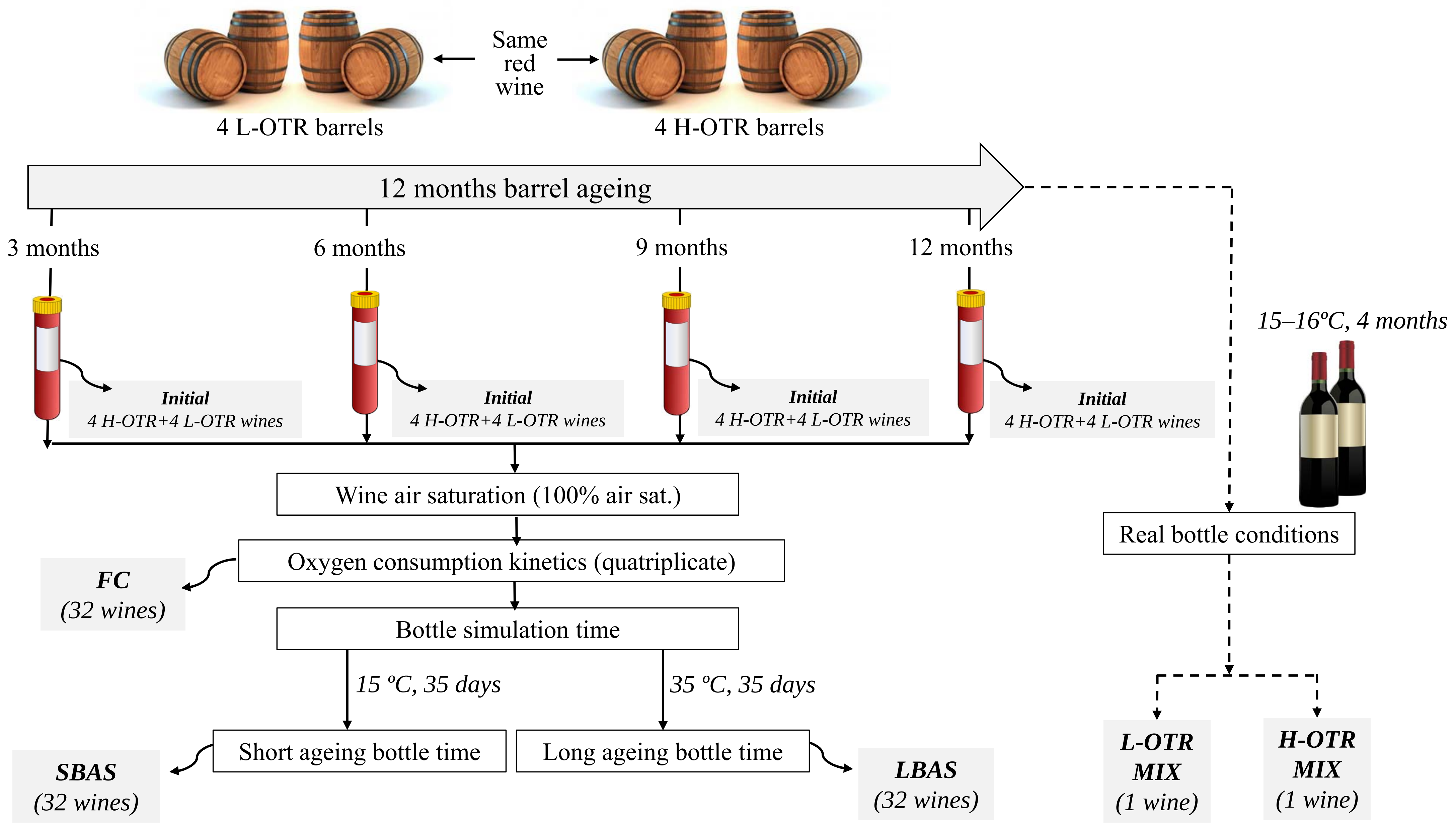

Same red wine
4 L-OTR barrels
4 H-OTR barrels
12 months barrel ageing
3 months
6 months
9 months
12 months
Initial 4 H-OTR+4 L-OTR wines
Initial 4 H-OTR+4 L-OTR wines
Initial 4 H-OTR+4 L-OTR wines
Initial 4 H-OTR+4 L-OTR wines
Wine air saturation (100% air sat.)
Oxygen consumption kinetics (quatriplicate)
FC (32 wines)
Bottle simulation time
15 ºC, 35 days
35 ºC, 35 days
Short ageing bottle time
Long ageing bottle time
SBAS (32 wines)
LBAS (32 wines)
15–16ºC, 4 months
Real bottle conditions
L-OTR MIX (1 wine)
H-OTR MIX (1 wine)

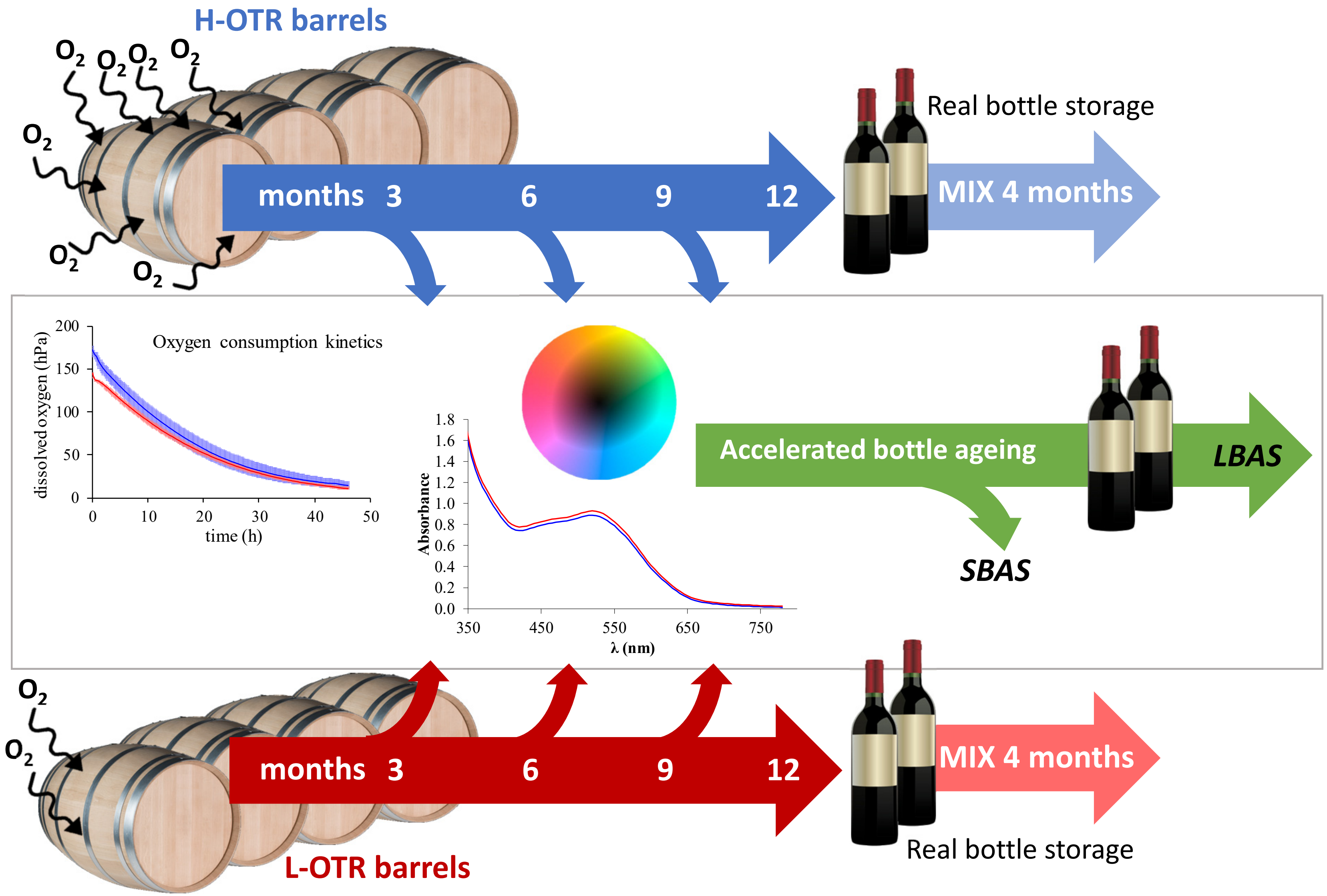
H-OTR barrels
O2
months 3 6 9 12
Real bottle storage
MIX 4 months
Oxygen consumption kinetics
dissolved oxygen (hPa)
time (h)
Absorbance
λ (nm)
Accelerated bottle ageing
LBAS
SBAS
months 3 6 9 12
MIX 4 months
Real bottle storage
L-OTR barrels